

IMPROVED FUZZY-C-MEANS FOR NOISY IMAGE SEGMENTATION

Moualhi Wafa and Ezzeddine Zagrouba

*Equipe de Recherche Systèmes Intelligents en Imagerie et Vision Artificielle
Institut Supérieur d'Informatique, Abou Raihane Bayrouni, 2080, Tunisia*

Keywords: Improved fuzzy-c-means (IFCM), Robustness, Noise, Spatial constraints, Gray constraints, Image processing.

Abstract: Magnetic resonance (MR) imaging is an important diagnostic imaging technique to early detect abnormal changes in the brain tissues. However, a serious limitation of the MR images is the significant amount of noise which can lead to inaccurate segmentation. In this paper, a robust segmentation method based on an improvement of the conventional Fuzzy-C-Means (FCM) by modifying its membership function is realized. A neighborhood attraction depending on the relative location and features of neighboring pixels is incorporated into the membership function to make the method robust to noise. Simulated and real brain MR images with different noise levels are used to demonstrate the superiority of the proposed method compared to some other FCM-based methods.

1 INTRODUCTION

Fuzzy-c-means clustering algorithm was highly effective for MRI segmentation among other clustering algorithms. However, one disadvantage of the conventional FCM is to only take care to pixels intensity and does not consider their location or any spatial information in image context which make it sensitive to noise. To compensate for the drawback of the conventional FCM, many researchers try to improve its effectiveness to noise. Tiliás and Panas post-processed the membership function to smooth the effect of noise (Tolias, 1998). Pham (Pham.a, 2001) modified the objective function to incorporate spatial context into the FCM. A parameter α is used as a tradeoff between the conventional FCM objective function and the smooth membership function. Pham and Prince (Pham.b, 1999) modified the FCM objective function by including a regularization term to estimate the spatially smooth membership function. Ahmed et al. (Ahmed, 2002) modified the objective function to allow the labeling of a pixel to be influenced by the labels of its immediate neighborhood. The main disadvantage of this method is that it computes the neighborhood term in each iteration step, which is very time-consuming. To overcome this problem, Chen and Zhang (Chen, 2004) proposed two algorithms based

on the mean-filtered image and median-filtered image which can be computed in advance to replace the neighborhood term in the above method. Finally, (Renjie, 2008) modified the FCM algorithm by integrating a regularization term in the objective function. The method includes bias field correction and contextual constraints over neighborhood spatial intensity distribution. All these methods with spatial constraints have been proven effective for noisy image segmentation. However, in their objective functions, there exists a parameter α used as a tradeoff between robustness to noise and effectiveness of preserving the details in the image. The value of α has a crucial impact on the performance of those methods. In other words, α has to be large enough to eliminate the noise and small enough to prevent the image from losing much of its sharpness and details. In order to overcome the problem of the selection of α and to improve the image segmentation performance, in this paper, we modify the conventional FCM by incorporating local spatial information in the membership function to take into account the spatial information in an image. The improved method is used to guarantee robustness to noise, preserve details for image and to avoid the empiric adjustment of the parameter α .

2 SPATIAL FUZZY CLUSTERING

FCM is an unsupervised clustering algorithm introduced by Bezdek (Bezdek, 1981). Let $X = \{x_i\}_{i=1}^N \subset \mathbb{R}^p$ is a data set, where p is the dimension of the studied feature space. The FCM is an iterative optimisation algorithm which minimizes the objective function J_m (1) with respect to the membership matrix $U = \{u_{ij}\}$ and to the set of cluster centers W .

$$J_m(U, W) = \sum_{j=1}^c \sum_{i=1}^N (u_{ij})^m d_{ij}^2 \quad (1)$$

with the following constraints:

$$\sum_{j=1}^c u_{ij} = 1, \forall i; 0 \leq u_{ij} \leq 1, \forall j, i; \sum_{i=1}^N u_{ij} > 0, \forall j \quad (2)$$

where u_{ij} represents the membership of pixel x_i to the j^{th} cluster, $W = \{w_1, w_2, \dots, w_c\}$ is the set of cluster centers, c is the total number of clusters and $m > 1$ is a fuzzy weighting exponent used to control the fuzziness of the resulting partition. The distance metric $d(x_i, w_j^{(t)})$ (3) measures the squared distance from x_i to a cluster center w_j using the norm metric $\|\cdot\|$ at the t^{th} iteration.

$$d_{ij} = \|x_i - w_j^{(t)}\| \quad (3)$$

The FCM objective function J_m can be minimized by iteratively using the following update equations:

$$u_{ij}^{(t)} = \frac{(\sum_{l=1}^c \frac{d_{il}^{-2}}{d_{il}^{(m-1)}})^{(t)} + \Gamma_{ij}^{(t)}}{\sum_{s=1}^c (\sum_{l=1}^c \frac{d_{il}^{-2}}{d_{il}^{(m-1)}})^{(t)} + \Gamma_{is}^{(t)}} \quad (4)$$

and

$$w_j^{(t)} = \frac{\sum_{i=1}^N (u_{ij}^{(t-1)})^m x_i}{\sum_{i=1}^N (u_{ij}^{(t-1)})^m} \quad (5)$$

with the following local spatial information term:

$$\Gamma_{ij}^{(t)} = \sum_{k \in N_i} \xi_{ik} u_{kj}^{(t-1)} \quad (6)$$

where N_i denotes the configuration of neighbors belonging into a local window (3×3) around x_i and the factor ξ_{ik} incorporates both local spatial relationship (called $\xi_{s,ik}$) and local gray level relationship (called $\xi_{g,ik}$) as presented below:

$$\xi_{ik} = \begin{cases} \xi_{s,ik} \times \xi_{g,ik} & i \neq k \\ 0 & i = k \end{cases} \quad (7)$$

where the i^{th} pixel is the center of the local window and the k^{th} pixel is a neighbor of the i^{th} pixel. Here, the definition of $\xi_{s,ik}$ is given by:

$$\xi_{s,ik} = \exp \frac{-(a_i - a_k)^2 + (b_i - b_k)^2}{|N_i|^2} \quad (8)$$

The relative location between the pixel i and its neighboring pixel k is calculated by $(a_i - a_k)^2 + (b_i - b_k)^2$ where (a_j, b_j) and (a_k, b_k) denote the coordinates of the pixels i and k . The $\xi_{s,ik}$ makes the influence of the pixels within the local window strongly dependent on their distance from the central pixel. The second factor defines the local gray level similarity measure $\xi_{g,ik}$ and presented as follows:

$$\xi_{g,ik} = \exp \frac{\|x_i - x_k\|^2}{\sum_{k \in N_i} \|x_i - x_k\|^2} \quad (9)$$

where x_i is the gray value of the central pixel i and x_k is the gray value of the neighbor pixel k . The $\|x_i - x_k\|$ is the intensity difference between the studied pixel i and its neighbor pixel k . The value of $\xi_{g,ik}$ should be large when the gray value of the k^{th} neighbors of x_i is close to the gray value of x_i and vice versa. The new factor ξ_{ik} incorporates both the local spatial relationship and the local gray level relationship and its value varies relatively to each pixel of the image. It can be determined automatically rather than empirically selected.

For convenience of notation later, we will name the FCM algorithm introduced by (Ahmed, 2002) A-FCM and the spatial fuzzy clustering algorithm IFCM and it can be summarized in the following steps.

Algorithm

1. Fix the number of clusters c ($2 < c < N$), given a priori knowledge, and the degree of fuzziness m .
2. Initialize randomly cluster centers $W^{(0)}$ and set ϵ to a very small value equals to 10^{-5} .
3. Calculate the initial membership matrix $U^{(0)}$ associated with the given cluster centers using (4) with the constraint $\Gamma^{(0)} = 0$.

Repeat

4. At the t^{th} iteration ($t=0, 1, 2, \dots$), compute the new cluster centers $W^{(t)}$ using (5).
5. Compute the new membership matrix $U^{(t)}$ using (4).

Until

6. $\|U^{(t+1)} - U^{(t)}\| < \epsilon$

3 RESULTS AND DISCUSSIONS

To verify the performance of the IFCM method we give some experiments to compare the proposed method with two other FCM-based methods as the conventional FCM and the A-FCM described above. Three types of images were employed for the evaluation of the IFCM which are a synthetic square

image, simulated brain images downloaded from Brainweb (Brainweb) and finally real MR images of brain tissues from IBSR (IBSR) and Whole Brain Atlas (WholeBrain).

3.1 Square Image

A synthetic square image consisting of 4 squares is generated. It contains uniformly distributed noise in the interval (-15,+15). Figure 1(a) shows a synthesized image with the corresponding gray values are 0 (upper left, UL), 100 (upper right, UR), 200 (low left, LL) and 250 (low right, LR) respectively. Figure 1(b), (c) and (d) show the segmentation results of FCM, A-FCM, and IFCM. Figure 1(b) and (c) show that neither FCM nor A-FCM can overcome the degradation caused by noise in the segmentation result. Figure 1(c) illustrates the drawback of A-FCM since the edge of the image is blurred. Only IFCM completely succeeds in segmenting the four classes as shown in figure 1(d) and clearly preserves edge information.

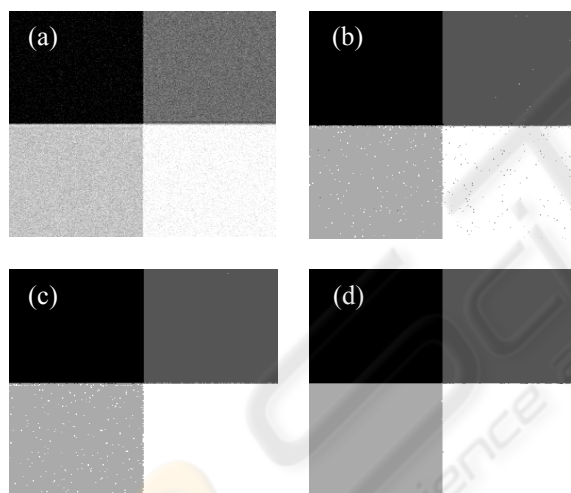


Figure 1: (a) Noisy synthetic square image. Segmentation results using (b) FCM; (c) A-FCM ($\alpha=0.75$); (d) IFCM.

3.2 Simulated MR Images

Brainweb provides a simulated brain database (SBD) including a set of MRI data to evaluate the performance of various segmentation methods where the truth is known. Thus, a simulated T1-weighted MR image was downloaded from Brainweb. The discrete anatomical model of the simulated image consisting of white matter, gray matter and cerebral spinal fluid (CSF) is shown from left to right in figure 2(a). A 7% noise level was applied to the simulated image and segmented into four clusters:

background, CSF, white matter and gray matter using the three methods but the background was neglected from the viewing results. A noisy segmentation result was obtained from FCM and a clear segmentation result was given by A-FCM and IFCM. In order to quantitatively evaluate the segmentation performance three evaluation parameters are used in this study. First, under segmentation $UnS = N_{fp}/N_n$ as the percentage of negative false segmentation. Second, over segmentation $OvS = N_{fn}/N_p$ as the percentage of positive false segmentation. Finally, incorrect segmentation $InC = (N_{fn} + N_{fp})/N$ as the total percentage of false segmentation where N is the total number of pixel in the image. Where N_{fp} is the number of pixels that do not belong to a cluster and are segmented into the cluster, N_{fn} is the number of pixels that belong to a cluster and are not segmented into the cluster, N_p is the number of all pixels that belong to a cluster and N_n is the total number of pixels that do not belong to a cluster. The performance evaluation parameters of the whole methods for the simulated T1-weighted MR image are computed in Table 1.

Table 1: Segmentation evaluation on simulated T1-weighted MR image.

Class	Parameters	A-FCM	FCM	IFCM
CSF	UnS(%)	4.38	8.62	3.83
	OvS(%)	61.36	66.64	76.61
	InC(%)	8.46	14.58	9.05
White matter	UnS(%)	3.37	2.09	2.54
	OvS(%)	36.57	45.54	37.55
	InC(%)	8.47	18.76	7.91
Gray matter	UnS(%)	2.68	1.79	2
	OvS(%)	57.61	82.35	60.43
	InC(%)	12.74	18.85	12.70
Average	UnS(%)	3.47	4.16	2.79
	OvS(%)	51.54	42.90	58.19
	InC(%)	9.89	17.66	9.88

To further demonstrate the performance of the IFCM method at dealing with noise, different levels (0%–9%) of noise were applied to the simulated T1-weighted MR image. The noisy images were segmented using the three segmentation methods. Figure 3 shows the InC obtained from FCM, A-FCM and IFCM for simulated image with different gaussian noise levels. An increase in the level of noise led to an increase of InC for all methods. Figure 3 shows that for different noise levels, A-FCM and IFCM methods had a similar performance described by the InC parameter. However, the FCM

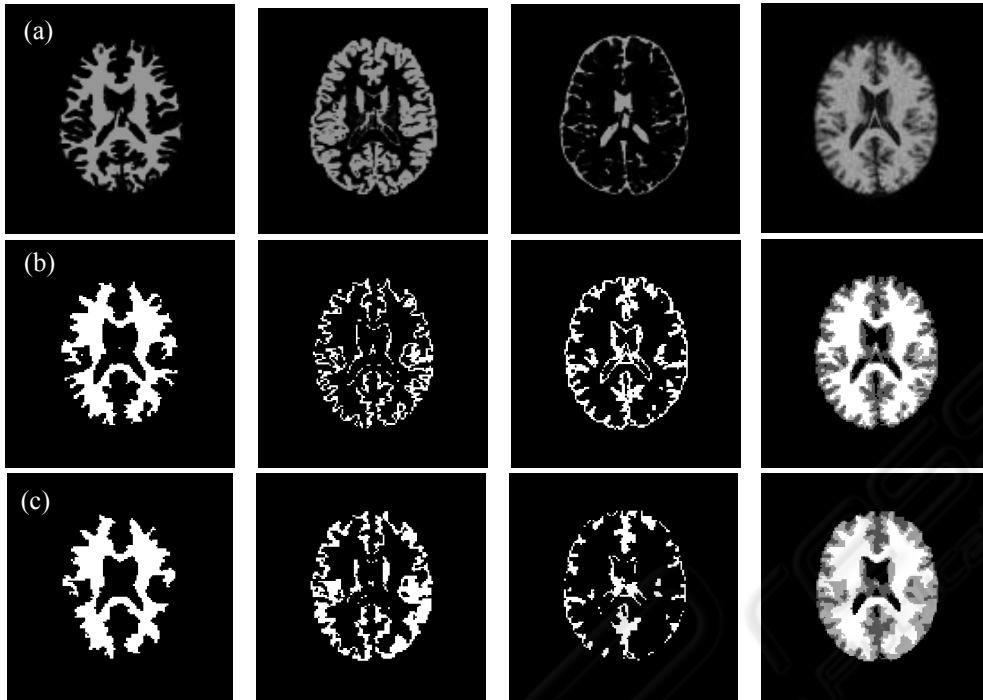


Figure 2: Simulated T1-weighted MR image. (a) Discrete anatomical model (from left to right) white matter, gray matter, CSF, and original image with 7% noise. Segmentation result using (b) A-FCM ($\alpha=0.75$); (c) IFCM.

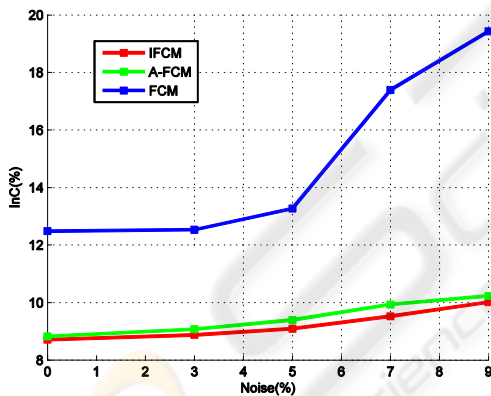


Figure 3: Variation of the InC with different noise levels.

method had a highest InC value and was less convincing in segmentation especially above 5% noise. The results for A-FCM and IFCM were close and both exhibited robustness to noise and reduced InC significantly within different noise levels. However IFCM had a lower InC and was more convincing in segmentation.

3.3 Real MR Images

A further experimentation for the all segmentation methods was given for real MR images in order to demonstrate the effectiveness of the IFCM method to

eliminate the noise. To this aim, a real coronal T1-weighted image was downloaded from IBSR by the Center for Morphometric Analysis at Massachusetts General Hospital. The web provides manually guided expert segmentation results along with brain MRI data for evaluation of segmentation methods.

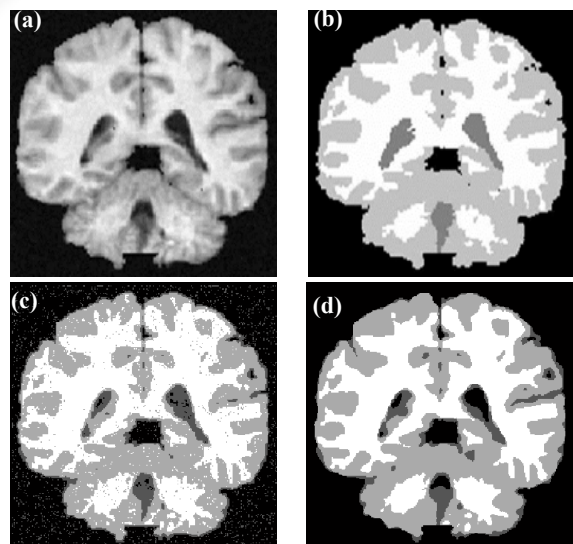


Figure 4: T1-weighted MR image from IBSR. (a) Original image with 3% noise. (b) Manual segmentation result. Segmentation result of FCM (c) and IFCM (d).

Figure 4(a) shows the original 25th slice of the image with 3% Gaussian noise and Figure 4(b) shows the manual segmentation result provided by the web. The manual segmentation result included four classes, CSF, gray matter, white matter, and others. The number of class of the original image is then fixed to four. Table 2 lists the evaluation parameters for the whole segmentation methods. The IFCM showed a significant improvement over the FCM and the A-FCM methods and completely eliminated the effect of noise.

Table 2: Evaluation on T1-weighted MR image.

Class	Parameters	A-FCM	FCM	IFCM
CSF	UnS(%)	3.20	5.22	4.70
	OvS(%)	59.94	45.88	61.37
	InC(%)	6.15	7.33	7.65
White matter	UnS(%)	15.48	5.41	2.66
	OvS(%)	2.74	12.47	14.52
	InC(%)	11.78	7.46	6.10
Gray matter	UnS(%)	2.25	6.82	6.75
	OvS(%)	43.50	20.86	22.30
	InC(%)	16.22	11.58	12.01
Average	UnS(%)	16.57	5.81	4.70
	OvS(%)	35.39	22.24	32.79
	InC(%)	11.38	8.79	8.58

A further example of real MR images is a real T1-weighted image with random gaussian noise. The preprocessing step including nonbrain region removal was applied to this image before segmentation. The segmentation results are shown in Figure 5. The IFCM method shows a superior performance than the FCM.

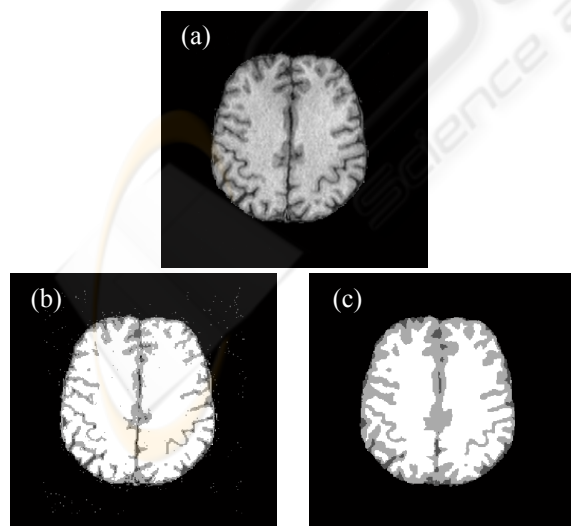


Figure 5: T1-weighted MR image with uniform noise from Brain whole. (a) Original brain only image. (b) From left to right: segmentation results of FCM and IFCM.

4 CONCLUSIONS

Clinically acceptable segmentation performance is difficult to achieve for magnetic resonance images because it generally contain unknown noise. Conventional FCM is based only on the pixel intensities which are not robust to segment noisy images. To overcome this shortcoming, an attraction between neighboring pixels is considered in this paper. In our proposed IFCM algorithm each pixel attempts to attract its neighboring pixels toward its own cluster during clustering. Preliminary results show that our method outperforms the FCM on the segmentation of noisy images.

REFERENCES

- Tolias, Y. A. and Panas, S. M., 1998. On applying spatial constraints in fuzzy image clustering using a fuzzy rule-based system," *IEEE Signal. Process. Lett.*, pp. 245–247.
- Pham.a, D. L., 2001. Spatial models for fuzzy clustering, *Comput. Vis. Imag. Understand.*, pp. 285–297.
- Pham.b, D.L., Prince, J.L, 1999. An adaptive fuzzy c-means algorithm for image segmentation in the presence of intensity inhomogeneities, *Pattern Recognition Letters*, pp. 57-68.
- Ahmed MN, Yamany SM, Mohamed N, Farag AA, Moriarty T, 2002. A modified fuzzy c-means algorithm for bias field estimation and segmentation of MRI data. *IEEE Trans Med Imaging*, pp. 193–202.
- Chen, S.C., Zhang, D.Q, 2004. Robust image segmentation using FCM with spatial constraints based on new kernel-induced distance measure, *IEEE Trans. Syst. Man Cybern. B*, pp.1907–1916.
- Bezdek, J. C., 1981. *Pattern Recognition with Fuzzy Object Function Algorithms*. New York: Plenum.
- Renjie, H., Sushmita D., Balasrinivasa R. S., Ponnada A. N., 2008. Generalized fuzzy clustering for segmentation of multi-spectral magnetic resonance images. *Comput Med Imaging Graph*, pp. 353-366.
- BrainWeb (Online). www.bic.mni.mcgill.ca/brainweb/
- IBSR (Online). www.cma.mgh.harvard.edu/ibsr/
- Whole Brain (Online). www.med.harvard.edu/AANLIB/